University of Thi_Qar Journal for Engineering Sciences ISSN 2075-9746
http://www.doi.org/10.31663/tqujes.10.1.354(2019)
Vol10 No.1 (May 2019)
Available at http://jeng.utq.edu.iq
engjrnal@jeng.utq.edu.iq

Prediction of the Shear Strength of Concrete T-Beams Using Artificial Neural Networks Model

Asst. Lecture Roaa Talib Abd

Directorate of education vocational education/ Al Hawra Preparatory School

Abstract

This paper presents an application of artificial neural network (ANN) to develop a model for predicting the shear strength of T-beams. The required data has been taken from literature. Statistical tools like mean, standard deviation (SD), correlation coefficients (R) and mean absolute error (MAE) are adopted to verify the ANN model against the experimental results obtained from the literature and with the existing empirical codes. The produced ANN model is utilized to carry out a parametric analysis to study the impact of the multiple parameters on the shear strength of T-beams. The parameters were shear span to depth ratios, effective depth, shear reinforcement, flange thickness, compressive strength of concrete, longitudinal steel ratio, flange width and web width. The outcomes of the parametric study show excellent trend agreement with the experimental database which emphasizes the statistical results. The overall analysis shows that the ANN model is more accurate than the guideline equations with respect to the experimental results and can be applied satisfactorily within the range of parameters covered in this study.

Keywords: Concrete; T-beams; Shear strength; Artificial neural networks; Parametric study.

1. Introduction

Although a number of researches have been conducted to estimate the shear strength of reinforced concrete beams for the last century, it is still hard to well predict actual shear strength because of shear behavior of reinforced concrete beams are very complicated due to many parameters such as concrete compressive strength, stirrup ratio, shear span-to-depth ratio, longitudinal reinforcement ratio, dimensions of the flange part of slab and so on [1, 2, 3, 4, 5, 6, 7, 8]. On evaluating shear strength of reinforced concrete beams, the shear design provisions around the world, such as American concrete institute and Canadian Standards Association, are much different from each other in the theoretical basis, specifically for reinforced concrete beams with stirrups [9, 10].

The objectives of this study are summarized as follows:

- Develop an artificial neural network model which can predict the shear strength of T-beams.
- Compare the predicted strength of T-beams using the trained artificial neural network model with those calculated from some well-known equations.
- Carry out a parametric study using the proposed model for the parameters affecting the shear strength of T-beams.

2. Related works

Recently, many researchers apply artificial neural network as a powerful tool to solve complex problems in civil engineering studies like predicting compressive strength of confined concrete [11], the strength of recycled aggregate concrete [12] and axial strength of composite column [13].The following are the more specific related works:

Sanad and saka (2001) use the artificial neural network in predicting the ultimate shear strength of reinforced –concrete deep beams. The determined from ACI code method, strut-and-tie method and Mau-Hsu method. [14]

Ashour et al. (2003) performed an empirical modelling of shear strength of reinforced concrete deep beam by genetic programming, which is a form of artificial intelligence. Good agreement between the model predictions and experiments has been achieved. [15]

Arafa et al (2011) applied to develop two models for predicting the ultimate shear strength of reinforced concrete deep beams for Normal Strength Concrete (NSC) and High Strength Concrete (HSC). The predicted shear strength values was compared with the experimental values and with the calculation from ACI code and achieve good agreements. [16]

Amani and Moeini (2012) used the Artificial Neural Network (ANN) and the Adaptive Neuro-Fuzzy Inference System (ANFIS) to predict the shear strength of Reinforced Concrete (RC) beams, and the models are compared with American Concrete Institute (ACI) and Iranian Concrete Institute (ICI) empirical codes. The models provides better prediction for shear strength. [17]

Vahidi and Rahimi (2016) developed a harmony search (HS) algorithm in ANN models. The model was validated and tested by 30 deep beams with opening. Comparisons between the predicted values and 30 test data showed that the developed ANN model resulted in improved statistical parameters with better accuracy than other existing equations. [18]

3. Shear behavior of beams

3.1. Beams without shear reinforcement

While the principal tensile stress at any point reaches the tensile strength of concrete, a crack will occur and open normal to the direction of the principal tensile stress or in a parallel direction to the principal compressive stress. Hence, concrete members subjected to shear forces at ultimate load regularly have inclined cracks named diagonal cracks or shear cracks. Inclined cracks can be started in the web of beams where is proved to be the greatest shear stress region and named web shear cracks. Inclined cracks formed from former flexural cracks are called flexure-shear cracks as shown in Figure (1). [19]

performance of the neural network in predicting the shear strength is much more accurate than those

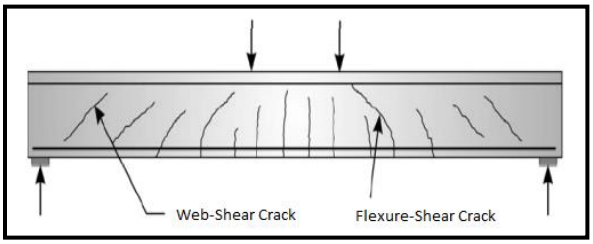

Figure (1) Types of inclined cracks.

The type of failure caused by these cracks, habitually in a very brittle and abrupt way, is termed diagonal failure or shear failure. Usually, there are five different forms of failure caused by diagonal cracks depending on the dimensions, geometries, kind of loading, amount of longitudinal reinforcement and structural characteristics of concrete members as shown in Figure (2), the failure forms are:

1) Diagonal tension failure.
2) Shear compression failure.
3) Shear tension failure.
4) Web crushing failure and.
5) Arch rib failure. [20]

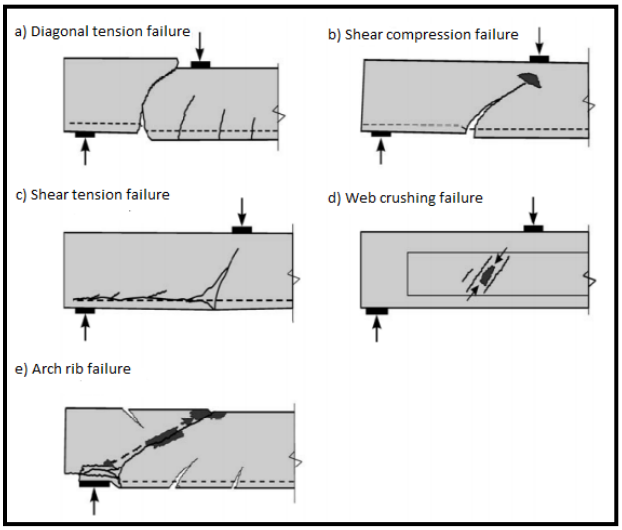

Figure (2) Forms of shear failure of concrete beams.

3.2. Beams with stirrups

The crack pattern of slender rectangular beams with stirrups is similar to that of beams without stirrups. In both cases of beams, the critical crack typically includes two branches, which are developed in the

same region of the beams. It is rational to consider the cause of formation of the second branch of the critical diagonal crack, as well as the corresponding cracking load, are the same in both cases. Up to the formation of the second branch of the critical crack, the effect of stirrups can be negligible. By the increase in the second branch of the critical crack and the strength of the beam, the stirrups are taking action. The continuous opening of the second branch, from the tip of the first branch towards the load point, requires a continuous and gradual increase of the concrete shear force V_{ccr} at the beginning of the second branch to balance the grown force V_s of stirrups. The concrete shear force at the end of the second branch remains unchanged.

Furthermore, the opening of the second branch of critical crack causes an increase in ΔV_d of the shear force of the longitudinal steel bars. Thus, the forces acting at failure on the part of the beam above critical diagonal crack can be regarded to be those shown in Figure (3). Taking into account that the shear force V_{cr} at the beginning of cracking of the second branch of the critical crack is equal to the sum ($V_{dcr} + V_{ccr}$), then from the vertical equilibrium of forces acting on the portion of the beam , thus V_u equal to the sum ($V_{cr} + V_s + \Delta V_d$). [21]

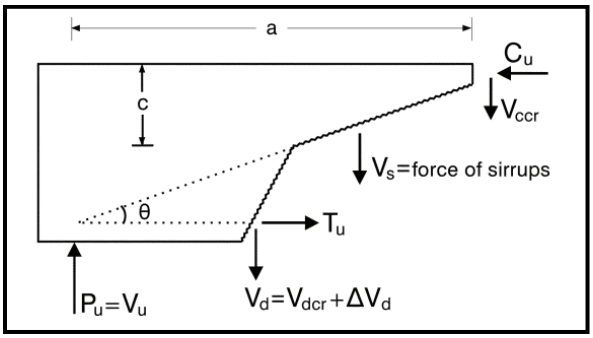

Figure (3) Forces on portion of beam with stirrups above critical diagonal crack at failure.

4. Prediction of shear strength of concrete

4.1. Empirical codes

4.1.1. American concrete institute (ACI 318-14)[9]

For reinforced concrete beams with stirrups and with rather large shear span to depth ratio, ACI 318-14(2014) simply evaluates shear strength as sum of concrete and stirrup contributions (V_c and V_s, respectively). The predicted shear strength are presented in Table A2. In preparing the values of this table, the expression of the code is used without including in it any safety factor. Thus, for ACI Code predictions (in SI units)

$$V_c = \left(0.16 * \lambda * \sqrt{f_c'} + 17 \ * \rho * \frac{V_u\, d}{M_u} \right) b_w d \leq 0.29 * \sqrt{f_c'} \ * b_w d \quad (1)$$

$$where \quad \frac{V_u\, d}{M_u} \leq 1$$

$$V_s = A_v f_{yv} d/s \quad (2)$$

$$V = V_c + V_s \quad (3)$$

$$\rho_v = A_v/b_w s \quad (4)$$

$$V = b_w d \left(0.16 * \lambda * \sqrt{f_c'} + 17 \ * \rho * \frac{V_u\, d}{M_u} + \rho_v f_{yv} \right) \quad (5)$$

Where λ is the factor to account for low-density concrete and equal 1.00 for normal density concrete, f_c' is the compressive strength of concrete , V_u is the factored shear strength at the section, M_u is the factored moment at the section, b_w is beams web width in mm, d effective depth of beams in mm, A_v is the area of vertical stirrups within a distance s, Where ρ is the ratio of main tension reinforcement, ρ_v is the ratio of shear reinforcement, f_{yv} is the yield strength of shear reinforcement. As Shown in Figure (4).

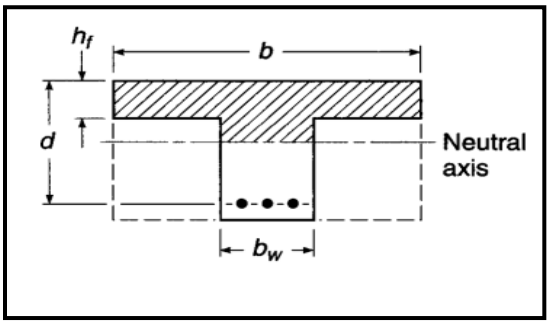

Figure (4) Cross section of T-beam.

4.1.2. Canadian Standards Association CSA A23.3 (2014)[10]

CSA A23.3 (2014) is based on the variable truss angle model and the effect of deformation of web due to flexure on evaluating the contribution of concrete and stirrups for shear strength since it was developed through simplifying the Modified Compression Field Theory, which can consider compatibility and equilibrium together.

$$V_c = \emptyset_c \lambda \beta \sqrt{f_c'}\, b_w d_v \quad (6)$$

$$V_s = \emptyset_s A_v f_y d_v \cot\theta / s \quad (7)$$

The total shear strength (V) is sum of V_c and V_s, thus

$$V = b_w d_v \left(\emptyset_c \lambda \beta * \sqrt{f_c'} + \emptyset_s \rho_v f_y \cot\theta / s\right) \quad (8)$$

Where θ is the Main diagonal angle which shall be taken as 35° (for f_c' does not exceed 60 MPa), β is the factor accounting for shear resistance of cracked concrete, equal 0.18, $\emptyset_c$ is the resistance factor for concrete, equal 0.65, $\emptyset_s$ is the resistance factor for non-prestressed reinforcing bars, equal 0.85, λ is the factor to account for low-density concrete, equal 1.00 for normal density concrete, d_v is the effective shear depth.

4.1.3. Ioannis et al (2006) [22]

They presented a theory for the shear resistance of reinforced concrete T-beams. The theory was an extension of the theory of slender rectangular beams. It gave an expression showed that the shear strength of slender T-beams is a superposition of the shear strength of T-beams with and without shear reinforcement. An effective width suitable for predicting the shear strength of T-beams is used in this expression. Also, a correction factor to account for the size effect is included in that expression. This expression is a generalized one, valid for T-beams as well as for rectangular beams and it is:

$$V = \left[\left(1.2 - 0.2\frac{a}{d}d\right)\frac{b_{ef}}{b_w} \times \frac{c}{d} f_{ct} + \left(0.5 + 2.5\frac{a}{d}\right)\rho_v f_{yv}\right] b_w d \quad (9)$$

The effective width b_{ef} is given by:

$$b_{ef} = b_w\left[1 + 0.5 \times \frac{h_f}{d}\left(\frac{b}{b_w} - 1\right) / \frac{c}{d}\right] \quad (10)$$

The depth c of the compression zone is given by the positive root of the following equation:

$$\left(\frac{c}{d}\right)^2 + \left[1.5\frac{h_f}{d}\left(\frac{b}{b_w} - 1\right) + 600\frac{\rho + \rho'}{f_c'}\right] \times \frac{c}{d} - 600\frac{\rho + \rho'\frac{d'}{d}}{f_c'} = 0 \quad (11)$$

The splitting tensile strength of concrete (f_{ct}) is calculated from

$$f_{ct} = 0.3 f_c^{2/3} \quad (12)$$

Where, ρ is the ratio of main tension reinforcement, which equals $A_s / b_w d$, ρ' is the ratio of compression reinforcement which equals $A_s'/b_w d$, A_s is the area of tension reinforcement, A_s' is the area of compression reinforcement, a/d is the shear span to depth ratio, d is the effective depth of beam, d' is the effective depth to compression reinforcement and h_f is the flange thickness.

4.2. Artificial Neural Networks Models

Artificial Neural Networks get their name from nerve cells networks of the brain. They represent a simple version of the human brain. These computational models provide new directions to solve arising problems. In contrast to digital computers, ANNs involve parallel processing which gains computers an additional advantage to simultaneously process of large data. If enough data are available, ANNs are suitable for problems whose solutions require knowledge which is difficult to extract [23]. The neural networks have the ability to learn from experience without needing prior knowledge about the governing relationships and to generalize approximates of any functional relationship with reasonable accuracy. It has been reported that the patterns in a phenomenon can be recognized by the ability of ANN and overcome the difficulties due to the selection of the model form, such as linear, polynomial or power [24].

In many of proposed ANN-approaches, multilayer feed forward-back propagation neural network (MFBPNN) has been applied as shown in figure (5). Typical MFBPNN often has one or more hidden layers with a sigmoid transfer function which followed by an output layer of linear neurons [25]. Multiple layers of neurons with nonlinear activation functions permit the network to learn intricate nonlinear relationships between input and output vectors. Neurons in the hidden layer were connected to previous and next layer by network weights and biases. Application of training function would adjust the network weights

matrix for each epoch. There are three common backpropagation training algorithms, they are Levenberg Marquardt (trainlm), Bayesian Regularization (trainbr) and scaled conjugate gradient method (trainscg). [26]

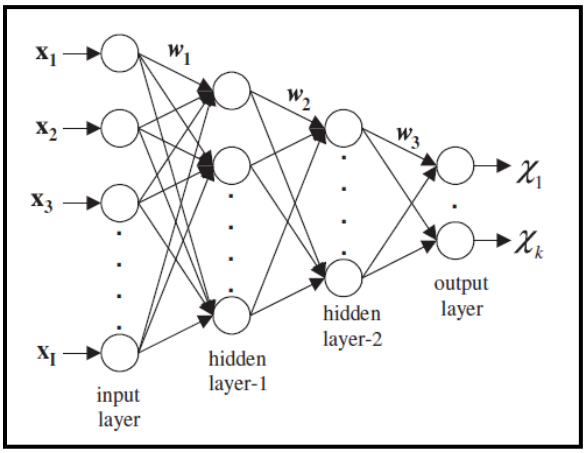

Figure (5) Artificial neural network with two hidden layers.

5. Methodology

In this study, an experimental database including 70 concrete T-beams has been investigated [22, 26 and 27]. Parameters of the experimental tests database and its range are presented in Table (1). The entire experimental database could be found in Appendix (A) table (A1).

Table (1). The range of parameters in the database.

Parameters	Range
Compressive strength of concrete(f_c')MPa	12 – 57
Beam′s web width (b_w) mm	50 - 300
Effective depth of beam (d) mm	240 - 399
Beam′s flange width (b) mm	200 - 960
Flange thickness (h_f) mm	0 – 102
Shear span to depth ratios (a/d)	3.33 - 10.4
Longitudinal steel ratio (ρ) %	0.49 - 8.34
ratio of shear reinforcement multiplied by the yield strength of shear reinforcement (ρ_v f_{yv}) MPa	0 - 3.46
Shear strength (V_n) kN	19 - 347.5

An (MFBPNN) model was developed to predict the shear strength of reinforced concrete T-beams and to investigate the interaction effects of the input parameters. The model has eight inputs which are compressive strength of concrete (f_c') in MPa, beams web width (b_w) in mm, effective depth of beams (d) mm, Beams flange width (b) in mm, flange thickness (h_f) in mm, shear span to depth ratios (a/d), longitudinal steel ratio (ρ) as percentage % and the ratio of shear reinforcement multiplied by the yield strength of shear reinforcement (ρ_v f_{yv}) in MPa. The output of the model was the shear strength in kN.

The network must be trained with an appropriate training function. The main objective of training the neural network is to specify the connection weights by reducing the errors between the predicted and actual target values to an adequate level. Through the minimization of the defined error function, which was Standard Mean Squared Error (Standard MSE), by updating the connection weights. Also, the data was normalization, the number of hidden layers, the number of hidden neurons and the type of transfer functions are chosen to get the best performance of the model. The training function was Bayesian regularization (trainbr) and the model consists of three hidden layers. The first and the third hidden layer with four neurons and the second hidden layer with seven neurons. The activation function of the hidden layers was the Log-sigmoid function (logsig). The model has one output layer with linear transfer function (purelin). The best training performance of the proposed ANN was at Standard MSE equals to $1.73*10^{-3}$ as shown in Figure (6). The network performance also has been checked for training, testing data set and for all data, as shown in Figures (7 a, b and c). A good agreement has been observed in the predicting values compared with the actual (targets) values.

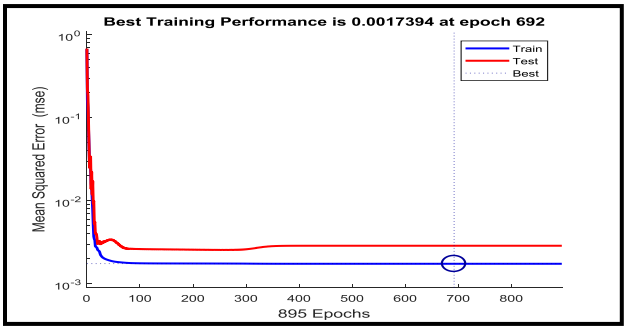

Figure (6) Convergence of the ANN for training and testing sets.

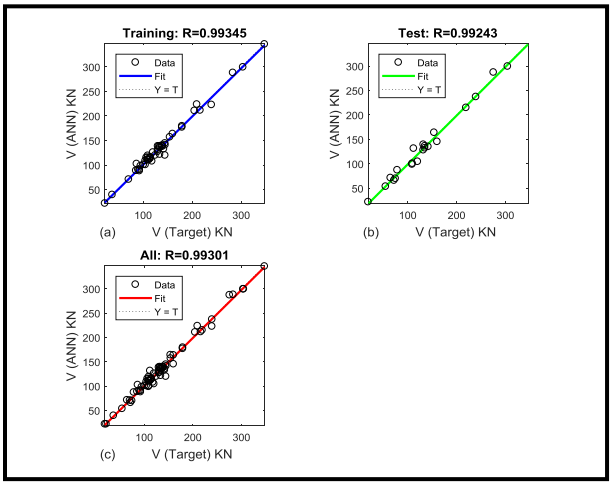

Figure (7) Comparison between ANN results and target results for (a) Training data set sets, (b) Testing data set and (c) All data.

6. Results and Discussions

6.1. Comparison between experimental and theoretical results

The experimental database was utilized to evaluate the precision of shear strength of proposed method (ANN) and to compare the ANN prediction with existing equations, the ratio (V_{th} /V_{exp}) was used (the whole results could be found in Appendix B). V_{th} and V_{exp} are the shear strength of T-beam based on prediction models and experimental works, respectively. Mean and standard deviation (SD) of the shear strength ratio (V_{th} /V_{exp}) are calculated. In addition to that, Correlation coefficients (R) and Mean Absolute Error (MAE) between predicted and experimental shear strength are used as another comparing tool. If the mean value of (V_{th} /V_{exp}) and Correlation coefficients (R) are close to one and the standard deviation and Mean Absolute Error (MAE) is small, it will give an indication of what the good ability to generalize the information. The results showed, according to the four indicators, that the best prediction is achieved by the proposed ANN model so it can be used to obtain more accurate results. As shown in Table (2), Figure (8) and appendix (A) Table (A2).

Table (2). Comparison between existing equations and the Proposed ANN.

The Indicator	ACI 318-14	CSA A23.3	Ioannis et al	Proposed ANN
Mean of V(th/exp)	0.6409	0.6636	1.0163	1.0023
Standard deviation of V(th/exp)	0.1696	0.1680	0.0910	0.0633
Correlation coefficients (R) with Experimental V	0.8977	0.9445	0.9851	0.9930
Mean Absolute Error (MAE)	51.2617	41.4218	8.8700	5.4862

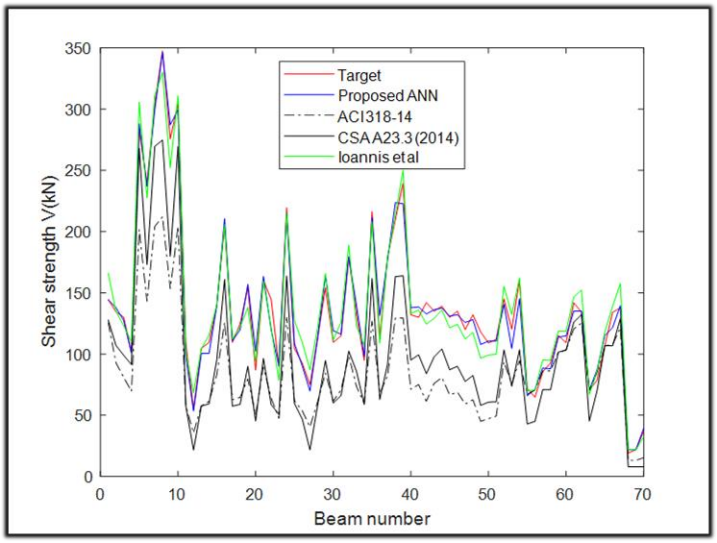

Figure (8) Comparison of experimental and predicted values for Proposed ANN,'ACI 318-14, CSA A23.3 (2014) and Ioannis et al.

6.2. Parametric analyses based on ANN

When the artificial neural network has been trained, a parametric analysis is used to study the impact of the multiple parameters on the shear strength of T-beams. The fundamental idea is to predict the effect of a range of values for only one variable while the remaining variables are kept constant and then investigate with a good trained ANN. The maximum and the minimum value of each parameter was summed and divided by two to get the constant value for the seven parameters

while the eighth one change from minimum to maximum exist values, that is for the input parameters to get its effect on the output parameter which is the shear strength.

In Figure (9) shear strength of concrete of T- beams is plotted versus shear span to depth ratios (a/d). It can be clearly seen from the figure that the increase in the ratios (a/d) leads the shear strength to decrease. It can be noticed from the Figure (10) and Figure (11) that the shear strength variation is nonlinear with both the effective depth of the T-beam (d) and ratio of shear reinforcement multiplied by the yield strength of shear reinforcement ($\rho_v f_{yv}$) and as the effects of (d) or ($\rho_v f_{yv}$) increases, the shear strength increases. It is recognized from the Figure (12) that flange thickness (h_f) has a very clear nonlinear effect on the shear strength of concrete T- beams. the relationship has a positive pattern with a rather fixed shear effect range of (h_f) from (60 to 80) mm. Figures (13) to (16) display a semilinear positive effects between shear strength of concrete T- beams and each of compressive strength of concrete (f_c'), Longitudinal steel ratio (ρ) %, Beams flange width (b) and Beams web width (b_w). Which is in general agreement with the experimental results and [9, 10 and 22] and that is a good validation check of the ANN in addition to the mentioned statistical results.

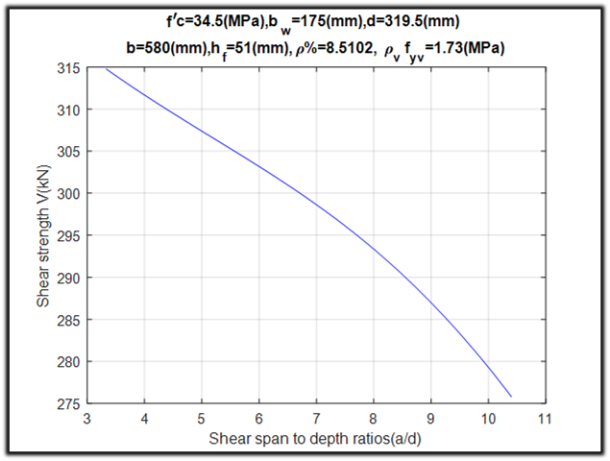

Figure (9) Effect the shear span to depth ratios (a/d) on shear strength of T beams.

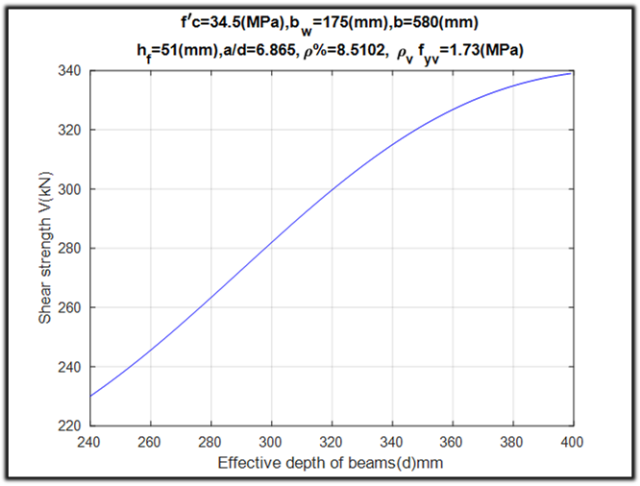

Figure (10) Effect the effective depth (d) on shear strength of T beams.

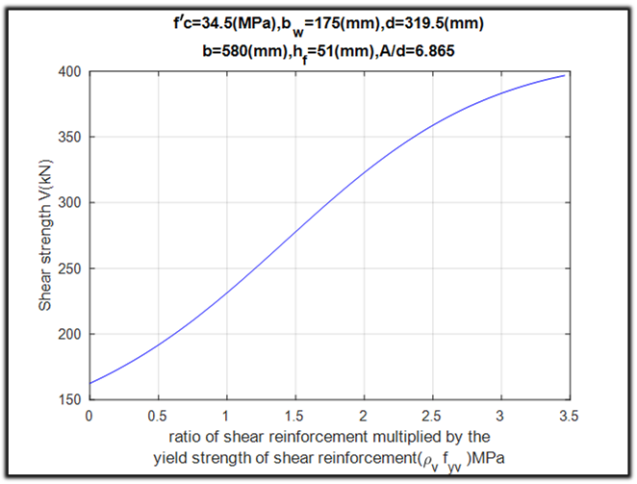

Figure (11) Effect the ratio of shear reinforcement multiplied by the yield strength of shear reinforcement ($\rho_v f_{yv}$) on shear strength of T beams.

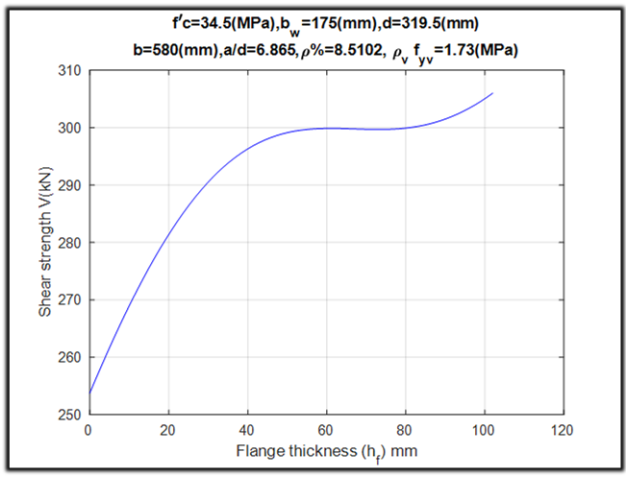

Figure (12) Effect the flange thickness (h_f) on shear strength of T beams.

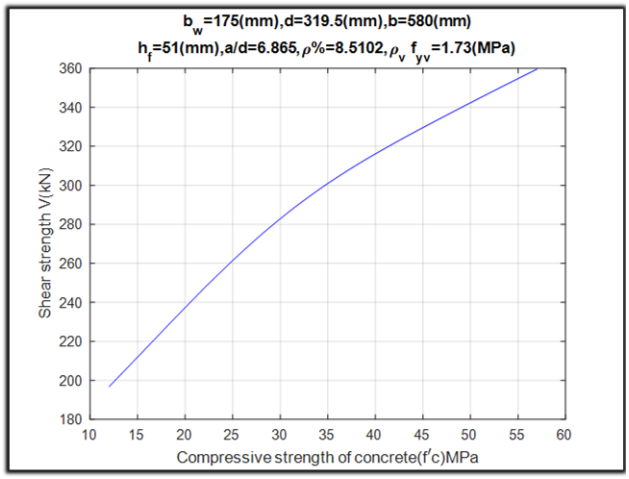

Figure (13) Effect the compressive strength of concrete (f_c') on shear strength of T-beams.

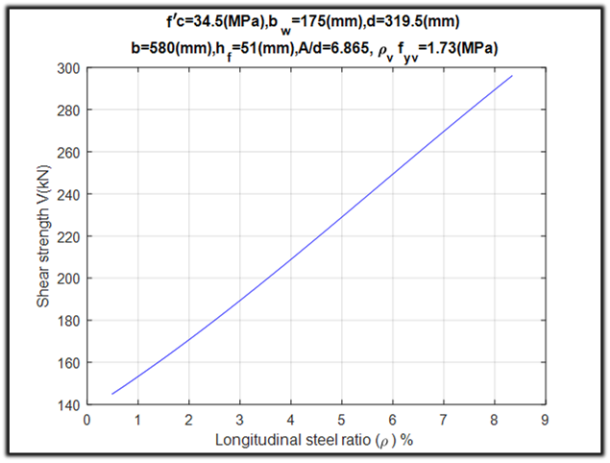

Figure (14) Effect the Longitudinal steel ratio (ρ) % on shear strength of T beams.

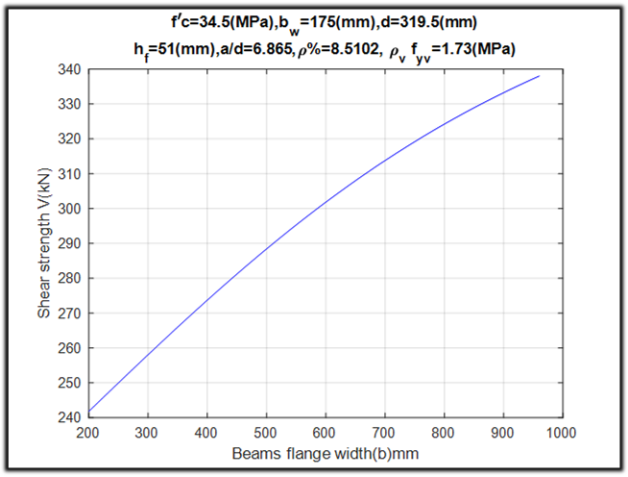

Figure (15) Effect the Beams flange width (b) on shear strength of T beams

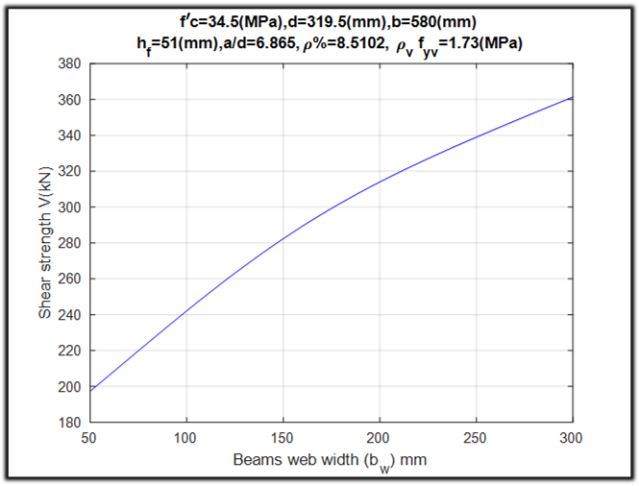

Figure (16) Effect the Beams web width (b_w) on shear strength of T beams.

7. Conclusion

This present study can be regarded as enrichment to a continuous effort to develop artificial neural network system for resolving the civil engineering problems. In this investigation, the model based on an Artificial Neural Network (ANN) is developed to predict the shear strength of T-beams. The database consists of a seventy tests data acquired from the review of the literature. The ANN model has eight inputs variables with one target variable which is the shear strength of concrete T-beams. The comparison between the experimental results and predictions

showed that the proposed ANN model well predicted the actual shear strength of reinforced concrete T-beams while the shear design provisions such as ACI 318-14 and CSA A23.3 showed notable scatter on the predictions. Also empirical equation for Ioannis et al is more accurate than the two shear design provisions, in the other hand, it less accuracy and more intricacy when compared with ANN model, so we can conclude that the multilayer feed forward back propagation neural network is the most suitable way to predict the shear strength of T-beams than the other three discussed methods.

8. References

[1] Kim, K. S. (2004), "Shear behavior of reinforced concrete beams and prestressed concrete beams", Doctorate thesis. Champaign, IL: Civil and Environmental Engineering, University of Illinois at Urbana-Champaign.

[2] Lee, S.C., Cho, J.Y. and Oh, B.H. (2010). "Shear behavior of large-scale post-tensioned girders with small shear span–depth ratio", ACI Structural Journal, 107(2), 137–145.

[3] Labib, E. L., Mo, Y. L., & Hsu, T. T. C. (2013)," Shear cracking of prestressed girders with high strength concrete", International Journal of Concrete Structures and Materials, 7(1), 71–78.

[4] Russo, G., Mitri, D., & Pauletta, M. (2013),"Shear strength design formula for RC beams with stirrups."Engineering Structures, 51, 226–235.

[5] Mofidi, A., & Chaallal, O. (2014),"Tests and design provisions for reinforced-concrete beams strengthened in shear using FRP sheets and strips", International Journal of Concrete Structures and Materials, 8(1), 117–128.

[6] Jeong, J.P. and Kim, W. (2014),"Shear resistance mechanism into base components: beam action and arch action in shear-critical RC members", International Journal of Concrete Structures and Materials, 8(1), 1–14.

[7] Chiu, C.K., Ueda, T., Chi, K.N., and Chen, S.Q. (2016),"Shear crack control for high strength reinforced concrete beams considering the effect of shear-span to depth ratio", International Journal of Concrete Structures and Materials, 10(4), 407–424.

[8] El-Sayed, A. K., and Shuraim, A. B. (2016),"Experimental verification of resistance-demand approach for shear of HSC beams,"International Journal of Concrete Structures and Materials, 10(4), 513–525.

[9] ACI Committee 318. (2014),"Building code requirements for structural concrete and commentary," ACI 318-14/ACIR-14. Farmington Hills, MI: American Concrete Institute.

[10] CSA A23.3-14. (2014), "Design of Concrete Structures, Canadian Standards Association", 5060 Spectrum Way, Suite 100, Mississauga, Ontario, Canada, L4W 5NG.

[11] Naderpour, H., Kheyroddin, A. and Amiri, G.G. (2010), "Prediction of FRP-confined compressive strength of concrete using artificial neural networks", Compos. Struct. 92, 2817–2829, http://dx.doi.org/10.1016/j.compstruct.2010.04.008.

[12] Khademi, F., Jamal, S.M., Deshpande, N. and Londhe, S. (2016), "Predicting strength of recycled aggregate concrete using artificial neural network, adaptive neuro-fuzzy inference system and multiple linear regression", Built Environ. 5 (2), 355–369.

[13] Ahmadi, M., Naderpour, H. and Kheyroddin, A. (2014), "Utilization of artificial neural networks to prediction of the capacity of CCFT short columns subject to short term axial load", Arch. Civ. Mech. Eng. 14, 510–517, http://dx.doi.org/10.1016/j.acme.2014.

[14] Sanad, A. and Saka, M.P. (2001) Prediction of ultimate shear strength of reinforced concrete deep beams using neural networks. J. Structural Eng., 127,818-828.

[15] Ashour, A.F., Alvarez, L.F. and Toropov, V.V. (2003) "Empirical modeling of shear strength of RC deep beams by genetic programming". Compute Structures, 81, 331-338.

[16] Arafa, M., Alqedra, M. and An-Najjar, H. (2011), "Neural Network Models for Predicting Shear Strength of Reinforced Normal and High-strength Concrete Deep Beams"Journal of applied Sciences, 11(2), 266-274.

[17] Amani, J. and Moeini, R. (2012), "Prediction of shear strength of reinforced concrete beams using adaptive neuro-fuzzy inference system and artificial neural network", Scientia Iranica, 19 (2), 242-248.

[18] Vahidi, E. K. and Rahimi, F. (2016), "Investigation of Ultimate Shear Capacity of RC Deep Beams with Opening using Artificial Neural Networks", Advances in Computer Science, 5 (4), No.22.

[19] NCHRP Report 549 (2005), "Simplified Shear Design of Structural Concrete Members"

[20] Raju, I. (2014), "Review on Shear Behavior of Reinforced Concrete Beam without Transverse Reinforcement" Journal of Engineering Research and Applications, 4 (4), 116-121.

[21] Zararis, P. D. (2003), "Shear Strength and Minimum Shear Reinforcement of Reinforced Concrete Slender Beams," ACI Structural Journal, 100, (2), 203-214.

[22] Ioannis, P. Z., Maria, K. K. and Prodromos, D. Z. (2006),"Shear Strength of Reinforced Concrete T-Beams", ACI Structural Journal, pp. 693-700.

[23] Zhang, B.E. Patuwo and M.Y. Hu (1998), "Forecasting with Artificial
Neural Networks",the State of the Art, International Journal of Forecasting , 14, 35-62.

[24] Tokar, A.S. and Johnson, P.A. (1999), "Rainfall–Runoff Modeling using Artificial Neural Networks", Journal of Hydrologic Engineering, 4(3), 232-239

[25] Beale, M.H., Hagan, M.T. and Demuth, H.B. (2017), "Neural Network Toolbox: User's Guide", MathWorks, Inc.

[26] Palaskas, M. N., Attiogbe, E. K. and Darwin, D. (1981), "Shear Strength of Lightly Reinforced T-Beams", ACI journal, Proceedings V. 78, No. 6, Nov.-Dec., 447-455.

[27] Kotsovos, M. D., Bobrowski, J. and Eibl, J. (1987), "Behaviour of Reinforced Concrete T-Beams in Shear", the Instruction of Structural Engineers, 65B, 1-10.

Appendix A

Table A1: experimental database including 70 concrete T-beams:

Beam NO	f_c' (Mpa)	b_w (mm)	d (mm)	b (mm)	h_f (mm)	a/d	ρ%	$\rho_v f_{yv}$ (Mpa)	V kN (exp)
1	22.6	300	300	300	0	3.5	1.39	0.57	144.5
2	23	150	300	300	75	3.5	2.78	1.16	134.5
3	23	100	300	300	75	3.5	4.17	1.73	130
4	23	50	300	300	75	3.5	8.34	3.46	101
5	15.4	160	375	960	80	3.33	4.4	2.51	283
6	15.4	160	375	960	80	3.33	4.4	1.53	239.5
7	17.4	160	375	960	80	3.33	4.4	2.51	303.5
8	24.9	160	375	960	80	3.33	4.4	2.51	347.5
9	24.9	160	375	960	80	3.33	4.4	1.53	275.5
10	17.4	160	375	960	80	3.33	4.4	2.51	304.5
11	27.9	152	254	610	76	3.36	1.25	0.58	109
12	28.1	152	254	610	76	3.36	1.46	0	54.7
13	27.5	152	254	610	76	3.36	1.46	0.58	104.6
14	32.5	152	254	610	76	3.36	1.95	0.58	109.5
15	33.7	152	254	610	76	3.36	1.46	1.15	139.7
16	25.8	152	254	610	76	3.6	4.16	2.25	204.7
17	27.4	152	254	610	76	3.46	3	0.58	109.5
18	31.3	152	254	610	76	3.6	4.16	0.58	124.6
19	20.2	152	254	610	76	3.6	4.16	1.15	154.4
20	28.2	152	254	610	76	3.36	4.16	0.38	86.8
21	37	152	254	610	76	3.6	4.16	1.15	160.2
22	30.7	152	254	610	76	3.6	4.16	0.58	144.6
23	12.8	152	254	610	76	3.36	4.16	0.58	89.9
24	33.4	152	254	610	76	3.6	4.16	2.25	219.4
25	33.2	152	254	610	76	7.2	4.16	0.58	104.5
26	32.7	152	254	610	76	7.2	4.16	0.38	92.6
27	28.4	152	254	610	76	3.6	4.16	0	74.8
28	30	152	254	610	76	5.4	4.16	0.58	113.5
29	32.1	152	254	610	76	5.4	4.16	1.15	154
30	34.4	152	254	610	76	3.36	4.16	0.58	109.5
31	54.1	152	254	610	76	3.36	4.16	0.58	114.8
32	57	152	254	610	76	3.6	4.16	1.15	179.3
33	12	152	254	610	76	3.6	4.16	1.15	132.1
34	31	152	254	610	76	3.36	1.46	0.58	94.8
35	27.6	152	254	610	76	3.6	4.16	2.25	216.3
36	43	152	254	400	80	5.4	4.16	0.58	112.1
37	24.2	152	254	400	80	3.6	4.16	1.15	179.3
38	31.8	152	254	400	80	3.6	4.16	2.25	209.6
39	30.2	152	256	400	80	3.6	4.16	2.25	239.4
40	33.1	110	298	400	80	3.5	3.84	1.42	132
41	31.7	110	298	400	80	3.5	3.84	1.51	130
42	34.9	110	298	400	80	3.5	3.84	1.2	142
43	23.4	110	298	400	80	3.5	3.84	1.53	135
44	25.1	110	298	400	80	3.5	3.84	1.64	139
45	25.1	110	298	400	80	3.5	3.84	1.32	130
46	25.7	110	298	400	80	3.5	3.84	1.37	135
47	23.6	110	298	400	80	3.5	3.84	1.15	120

48	25.4	110	298	400	80	3.5	3.84	1.23	132
49	25.1	110	298	400	80	3.5	3.84	0.77	118
50	25.2	110	298	400	80	3.5	3.84	0.82	109
51	26	110	298	400	80	3.5	3.84	0.82	112
52	43	150	285	600	80	3.5	1.45	1.07	145
53	40.7	150	285	600	80	3.5	1.94	0.65	120.2
54	43.1	150	285	600	80	3.5	1.94	1.07	160.2
55	32.8	190	374	610	102	4.14	0.69	0	72
56	32.7	190	394	610	102	3.92	0.66	0	64.7
57	32.6	190	390	610	102	3.97	0.66	0.22	85.5
58	33.1	190	388	610	102	4	0.67	0.22	92.6
59	26.3	190	392	610	102	3.96	0.66	0.51	115.1
60	28	190	393	610	102	3.94	0.66	0.51	109.2
61	32.2	190	395	610	102	3.92	0.66	0.67	141.8
62	38.1	190	371	610	102	4.18	0.7	0.76	134
63	32	190	399	610	102	3.88	0.49	0	70.5
64	30.8	190	394	610	102	3.92	0.49	0.22	78.6
65	30.6	190	391	610	102	3.96	0.5	0.53	106.6
66	29.7	190	393	610	102	3.94	0.94	0.53	134
67	29.4	190	395	610	102	3.92	0.93	0.71	137.7
68	40	50	240	200	65	10.4	5.23	0	19
69	40	50	240	200	65	10.4	5.23	0	22
70	40	50	240	200	65	3.33	5.23	0	37

Table A2: Comparisons of experimental and theoretical results:

Beam NO	Experimental V (kN)	ACI 318-14		CSA		Ioannis et al		Proposed ANN	
		V(kN)	V(th/exp)	V(kN)	V(th/exp)	V(kN)	V(th/exp)	V(kN)	V(th/exp)
1	144.5	125.83	0.871	127.880	0.885	166	1.149	144.280	0.998
2	134.5	92.81	0.690	107.005	0.796	134.9	1.003	137.935	1.026
3	130	81.00	0.623	98.945	0.761	123.1	0.947	127.404	0.980
4	101	69.49	0.688	91.370	0.905	110	1.089	100.945	0.999
5	283	201.75	0.713	267.946	0.947	305.6	1.080	287.983	1.018
6	239.5	142.95	0.597	173.010	0.722	227.3	0.949	236.965	0.989
7	303.5	204.12	0.673	269.506	0.888	310.9	1.024	299.312	0.986
8	347.5	211.98	0.610	274.679	0.790	330.0	0.950	346.050	0.996
9	275.5	153.18	0.556	179.743	0.652	252.0	0.915	287.067	1.042
10	304.5	204.12	0.670	269.506	0.885	310.9	1.021	299.312	0.983
11	109	57.46	0.527	57.628	0.529	101.5	0.931	98.787	0.906
12	54.7	35.60	0.651	21.551	0.394	68.3	1.249	53.513	0.978
13	104.6	57.64	0.551	57.473	0.549	104.0	0.994	100.430	0.960
14	109.5	61.42	0.561	59.331	0.542	115.6	1.056	100.524	0.918
15	139.7	83.11	0.595	95.285	0.682	140.2	1.004	139.404	0.998
16	204.7	125.83	0.615	160.903	0.786	205.6	1.004	210.537	1.029
17	109.5	62.80	0.574	57.435	0.525	112.4	1.026	110.833	1.012
18	124.6	64.54	0.518	58.899	0.473	121.9	0.978	119.756	0.961
19	154.4	79.75	0.517	89.957	0.583	138.1	0.894	156.860	1.016
20	86.8	50.33	0.580	45.276	0.522	94.0	1.083	102.349	1.179
21	160.2	89.56	0.559	96.414	0.602	159.6	0.996	163.438	1.020
22	144.6	64.20	0.444	58.680	0.406	121.3	0.839	119.751	0.828
23	89.9	47.35	0.527	50.699	0.564	78.5	0.873	90.682	1.009
24	219.4	130.15	0.593	163.748	0.746	215.0	0.980	214.733	0.979
25	104.5	61.78	0.591	59.579	0.570	127.4	1.219	108.571	1.039
26	92.6	53.79	0.581	46.935	0.507	109.8	1.186	90.385	0.976
27	74.8	40.50	0.541	21.665	0.290	87.0	1.163	69.737	0.932
28	113.5	61.28	0.540	58.421	0.515	121.8	1.073	113.397	0.999
29	154	84.45	0.548	94.718	0.615	165.8	1.077	163.863	1.064
30	109.5	61.48	0.561	59.998	0.548	111.2	1.016	119.072	1.087
31	114.8	70.68	0.616	66.056	0.575	126.0	1.098	116.138	1.012
32	179.3	98.62	0.550	102.378	0.571	189.0	1.054	179.284	1.000
33	132.1	73.38	0.555	85.768	0.649	122.7	0.929	139.351	1.055
34	94.8	59.64	0.629	58.789	0.620	107.0	1.129	97.994	1.034
35	216.3	126.91	0.587	161.611	0.747	208.0	0.962	211.400	0.977
36	112.1	67.96	0.606	62.813	0.560	108.7	0.970	131.351	1.172
37	179.3	82.37	0.459	91.684	0.511	179.4	1.001	176.824	0.986
38	209.6	129.29	0.617	163.179	0.779	213.0	1.016	223.539	1.067
39	239.4	129.41	0.541	163.875	0.685	250.0	1.044	222.681	0.930
40	132	71.09	0.539	95.012	0.720	133.1	1.008	137.792	1.044
41	130	75.07	0.577	99.351	0.764	135.8	1.045	138.426	1.065
42	142	61.36	0.432	83.902	0.591	124.4	0.876	132.674	0.934
43	135	75.96	0.563	97.673	0.724	129.1	0.956	136.158	1.009
44	139	80.82	0.581	104.090	0.749	135.8	0.977	137.550	0.990
45	130	66.66	0.513	87.154	0.670	121.4	0.934	130.829	1.006

46	135	68.88	0.510	90.006	0.667	124.2	0.920	132.100	0.979
47	120	59.14	0.493	77.632	0.647	112.3	0.936	125.711	1.048
48	132	62.68	0.475	82.494	0.625	117.6	0.891	128.060	0.970
49	118	45.02	0.382	58.045	0.492	96.5	0.818	107.793	0.913
50	109	47.24	0.433	60.726	0.557	99.1	0.909	110.522	1.014
51	112	49.30	0.440	60.999	0.545	99.8	0.891	110.446	0.986
52	145	93.61	0.646	103.373	0.713	155.3	1.071	140.771	0.971
53	120.2	75.45	0.628	73.583	0.612	132.2	1.100	104.453	0.869
54	160.2	94.68	0.591	103.407	0.645	162.2	1.012	145.233	0.907
55	72	67.13	0.932	42.854	0.595	69.7	0.968	65.879	0.915
56	64.7	70.64	1.092	45.077	0.697	70.8	1.094	71.160	1.100
57	85.5	86.09	1.007	70.871	0.829	95.1	1.112	88.529	1.035
58	92.6	86.18	0.931	70.846	0.765	94.8	1.024	87.931	0.950
59	115.1	101.21	0.879	101.549	0.882	118.6	1.030	113.858	0.989
60	109.2	103.43	0.947	103.091	0.944	118.5	1.085	114.740	1.051
61	141.8	120.57	0.850	126.030	0.889	146.6	1.034	134.942	0.952
62	134	125.20	0.934	132.312	0.987	152.2	1.136	135.039	1.008
63	70.5	70.24	0.996	45.157	0.641	67.1	0.952	70.636	1.002
64	78.6	84.53	1.075	70.338	0.895	85.5	1.088	87.115	1.108
65	106.6	106.72	1.001	106.844	1.002	118.0	1.107	115.098	1.080
66	134	107.71	0.804	106.746	0.797	138.9	1.037	121.544	0.907
67	137.7	121.42	0.882	128.883	0.936	157.6	1.145	139.539	1.013
68	19	13.17	0.693	7.992	0.421	21.8	1.147	21.855	1.150
69	22	13.17	0.599	7.992	0.363	21.8	0.991	21.855	0.993
70	37	15.35	0.415	7.992	0.216	32.4	0.876	39.286	1.062